Electronic Supplementary Material (ESI) for ChemComm.

Supplementary Information

One-step electrochemical synthesis of nitrogen and sulfur co-doped, high-quality graphene oxide

Khaled Parvez, Rosalba A. Rincón, Nils-Eike Weber, Kitty C. Cha, and Shyam S. Venkataraman*

Carbon Materials Innovation Center, BASF SE, 67056 Ludwigshafen, Germany

[*] E-mail: shyamsundar.venkataraman@basf.com

Experimental section:

Electrochemical synthesis of EGO: Graphite rod (diameter 3.05mm, Alfa Aesar) was used as both working and counter electrodes for the electrochemical exfoliation. The electrolyte for the exfoliation is prepared by dissolving 6.6 g of $(NH_4)_2SO_4$ in 50 mL water (i.e. concentration 1.0 M). The distance between the electrodes was 2 ± 0.5 cm and was kept constant throughout the electrochemical process. Electrochemical exfoliation was carried out by applying 1.0 A current using a Gamry potentiostat to the graphite electrodes. The current was kept constant for 2 h to complete the exfoliation process, where complete erosion of the working graphite electrode marks the end of the electrochemical processes. During the exfoliation process, nitrogen was continuously purged through the electrochemical system to flush away the hydrogen gas produced at the anode during electrochemical processes. After the graphite exfoliation was completed, the product was collected through a PTFE membrane filter with 0.2 μm pore size and washed with 500 mL Milli-Q water (resistance 18.2 MΩ) by vacuum filtration to remove the residual adsorption of electrolytes. The resultant exfoliated material was dispersed in water via ultrasonication for 20 min. The resulting dispersion was centrifuged at 5000 rpm for 5 min, to remove large agglomerates and particles. The total exfoliation yield was calculated using the mass ratio of the dried graphene powder and the starting graphite.

Commercial graphene oxide (Graphene Supermarket) prepared by chemical method was used for comparison.

Synthesis of Fe incorporated EGO: Composites of EGO with iron nanoparticles were synthesized by adding 20 mg of $Fe(NO_3)_3$ to 200 mg of EGO dispersion (0.5 mg/mL) and stirring the mixture for 1 h. The content of Fe (i.e. 20 wt%) in the composite was calculated with respect to the total mass of the EGO into the solution. Afterwards, the mixture was freeze dried to obtain the powder samples. The resulting solid was then annealed at 600 °C (ramp rate 10 °C/min) for 1 h under argon to form Fe-NS-EGO composites.

EGO thin film fabrication. Electrochemically exfoliated graphene oxide (EGO) thin film on flexible poly(ethylene terephthalate) (PET) substrate by vacuum filtration and dry transfer method.[1] Briefly, an EGO dispersion of 0.5 mg/mL in water was vacuum-filtered through a poly(tetrafluoroethylene) (PTFE) membrane followed by mechanically pressing the filtered film against a PET substrate. Afterwards, the PTFE membrane was peeled off, leaving the transferred EGO film on the substrate due to van der Waals interaction between the substrate and graphene.

Material characterization: The morphology and structure of the samples investigated by AFM (NT-MDT NTEGRA), HRTEM and SAED (Tecnai Osiris, FEI), SEM and EDX (Phenom ProX) and XRD (Bruker D4 X-ray scattering system with Ni-filtered Cu Kα radiation). Raman spectra was recorded with NT-MDT NTEGRA spectrometer (laser wavelength 488 nm) using a 100x optical objective with an average spot size of around 1μm. Chemical composition was determined by elemental analysis (STA 409, NETZSCH). The XPS measurements were obtained using a Scienta ESCA 200 spectrometer in ultrahigh vacuum. The samples for XPS measurements were carried out on a thin EGO powder film on double-faced adhesive tape. The four-point sheet resistance measurements were carried out with a linear four-point Jandel probe (1 mm needle spacing) and a Keithley 2400 Sourcemeter to obtain resistance values on 20 points covering the sample area. The average of these values (R) was then converted to a sheet resistance (R_s) using

$$R_s = \frac{\pi}{\ln 2} R$$

Electrocatalytic activity evaluation: The ORR activity of EGO samples were investigated using a rotating disk electrode (RDE). RDE measurements were performed using a CHI Electrochemical station (model 760D) in a conventional three-electrode electrochemical cell. Platinum coil and an Ag/AgCl/sat. KCl electrode were used as the counter and reference electrode, respectively. Prior to the use, a glassy carbon working electrode (5 mm in diameter) was polished with 0.05 μm alumina slurry to obtain mirror like surface, the washed with Milli-Q water and allowed to dry. The EGO ink for electrocatalytic ORR and OER experiments was prepared by dispersing 12 mg of EGO powder in 4 mL suspension consisting of 48.5 v/v % of ultrapure water, 48.5 v/v % isopropyl alcohol and 3 v/v % of Nafion 117® solution (Sigma Aldrich) *via* ultrasonication for 2 min. 10 μL of as-prepared EGO ink was drop casted on the surface of glassy carbon electrode, leading to a catalysts loading of 150 $\mu g/cm^2$. The electrodes were allowed to dry at room temperature before the measurements. Argon or oxygen saturated 0.1 M KOH was used as supporting electrolyte. All the potentials were converted to the reversible hydrogen electrode (RHE) scale.

An initial conditioning sweep was performed by cycling the electrode potential in the non-faradic region between 0.5 and 1.2 V *vs*. RHE, at a scan rate of 100 mV/s (100 cycles). Following the conditioning step, electrochemical impedance spectroscopy was recorded at open circuit potential (from 10 kHz to 0.1 Hz with 10 mV amplitude), in order to determine the cell uncompensated resistance and later perform iR correction of the potential. The oxygen reduction reaction (ORR) activity was evaluated by scanning the potential (linear sweep voltammetry, LSV) in the cathodic region (from 0 to -1 V *vs*. RHE) at a scan rate of 5 mV/s in the presence and absence of oxygen. The background current was determined in Ar-saturated environment without any rotation. For all the measurements in the O_2-saturated environment, the Ar background current was subtracted. The electrode was rotated at 1600 rpm, in order to avoid the accumulation of oxygen bubbles on the surface of the electrode.

The number of electrons transferred per O_2 molecule involved in the ORR at EGO electrodes was determined by the Koutecky-Levich (K-L) equation (Eq. 1-3):[2]

$$\frac{1}{J}=\frac{1}{J_L}+\frac{1}{J_K}=\frac{1}{B\omega^{0.5}} \qquad (1)$$

$$B=0.62nFC_o(D_o)^{2/3}v^{-1/6} \qquad (2)$$

$$J_K=nFkC_o \qquad (3)$$

Where J is the measured current density, J_K and J_L are the kinetic and diffusion-limiting current densities, ω is the angular velocity of the disk ($\omega = 2\pi N$, N is the linear roation speed), n is the overall number of electrons transferred in the oxygen reduction, F is the Faraday constant (96485 C/mol), C_o is the bulk concentration of O_2 (1.2×10^{-6} mol/cm^3), ν is the kinematic viscosity of the electrolyte (0.01 cm^2/s), D_o is the diffusion coefficient of oxygen (1.90×10^{-5} cm^2/s) and k is the electron transfer rate constant.

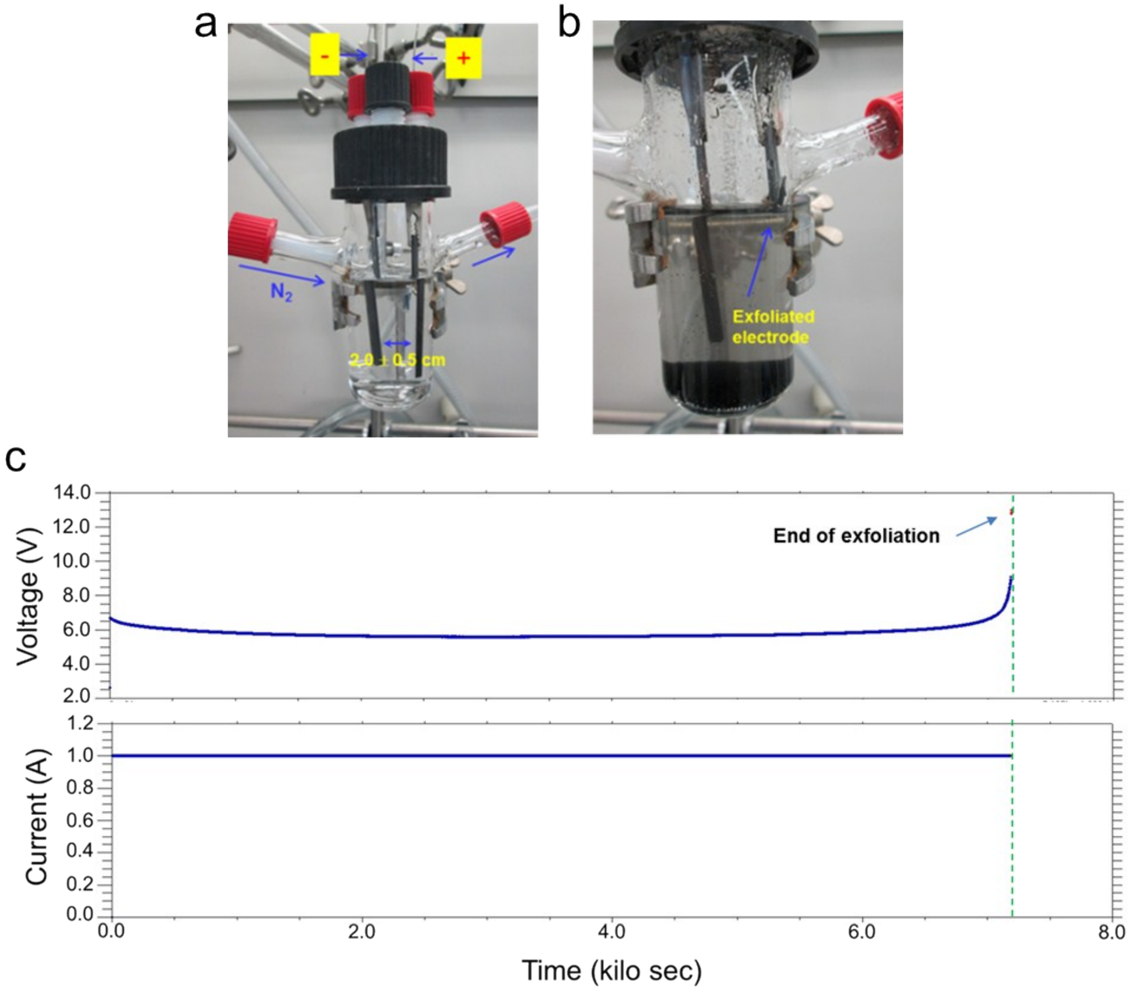

Fig. S1: Photographs of the graphite electrodes where, (a) before and (b) after electrochemical exfoliation. (c) Current-Voltage profile of the electrochemical exfoliation, where the end of the blue colored line marks the end of the exfoliation of graphite rod.

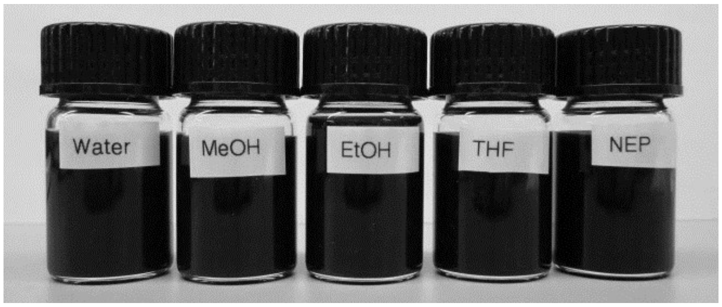

Fig. S2: Stable dispersion of EGO in various solvents

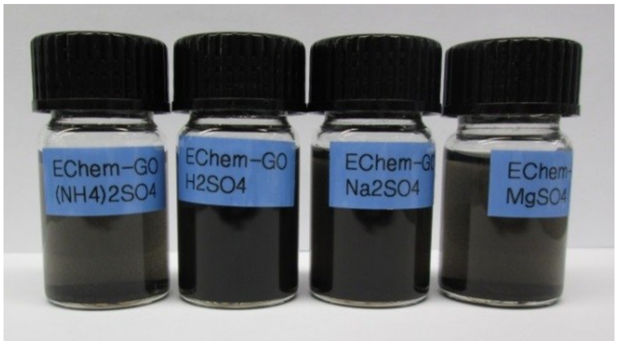

Fig. S3: Photograph of EGO dispersions in water obtained by electrochemical exfoliation of graphite rod in different electrolyte solutions such as, $(NH_4)_2SO_4$, H_2SO_4, Na_2SO_4 and $MgSO_4$.

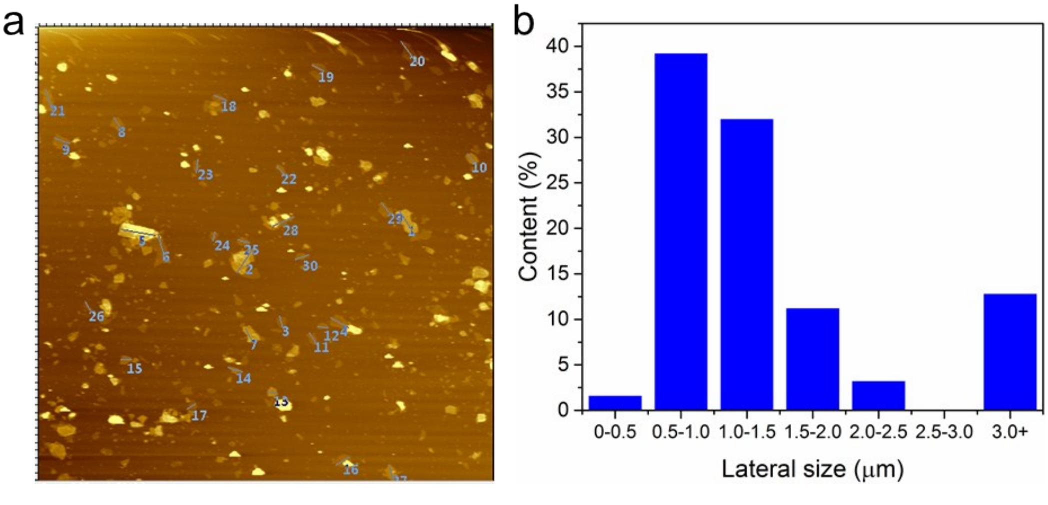

Fig. S4: (a) AFM image of EGO sheets on SiO_2 substrates. The numerical values and lines in the image represents the number of EGO flakes and their lateral dimensions used for flake size analysis, respectively. (b) Statistical flake size analysis of EGO obtained from (a).

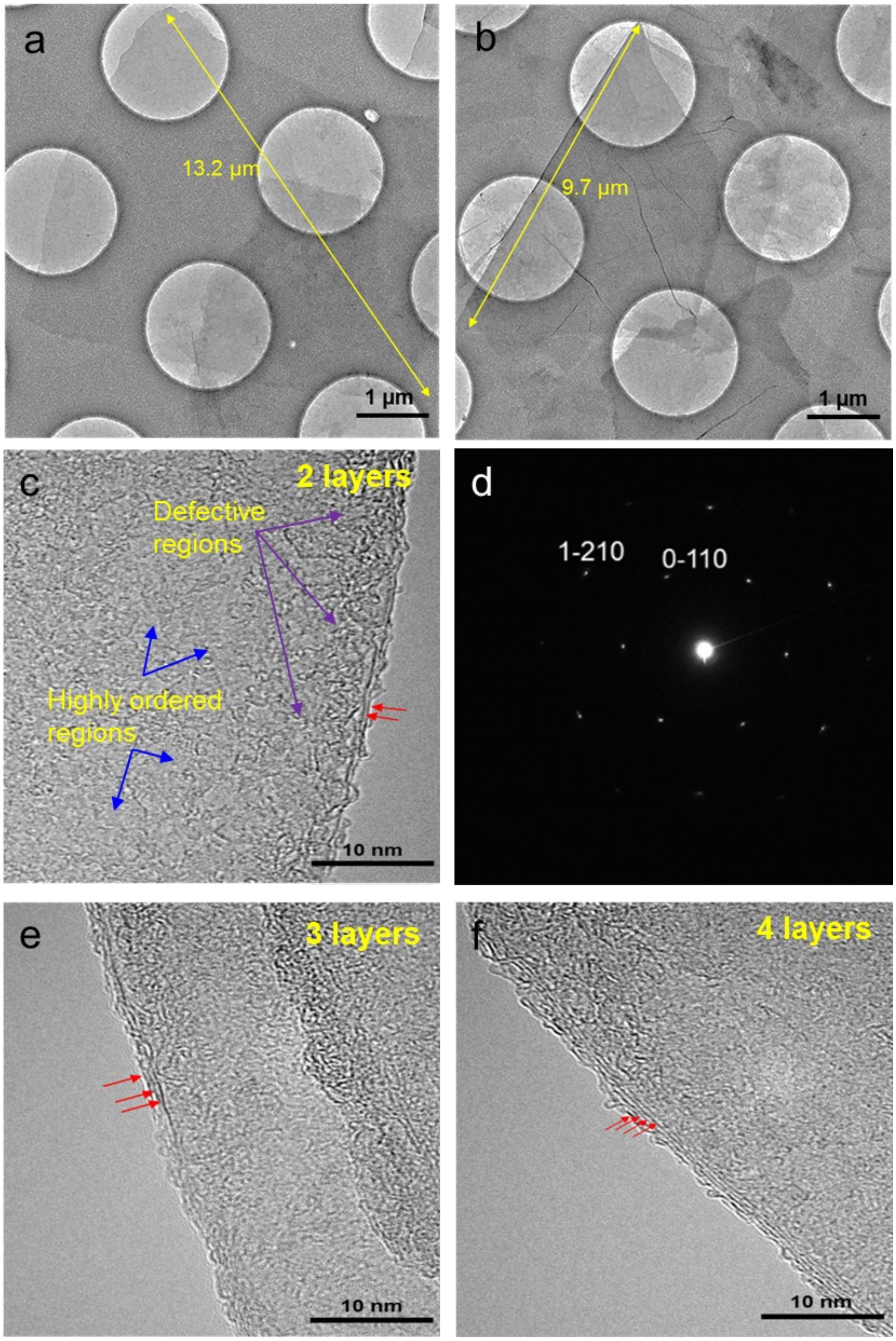

Fig. S5: (a) and (b) TEM image of large EGO sheets. (c) HRTEM image of a bilayer EGO. Highly-ordered and defective regions are indicated by blue and purple colored arrows, respectively (d) SAED pattern of a bilayer EGO (f) and (f) HRTEM images of a 3-layer and a 4-layer EGO, respectively.

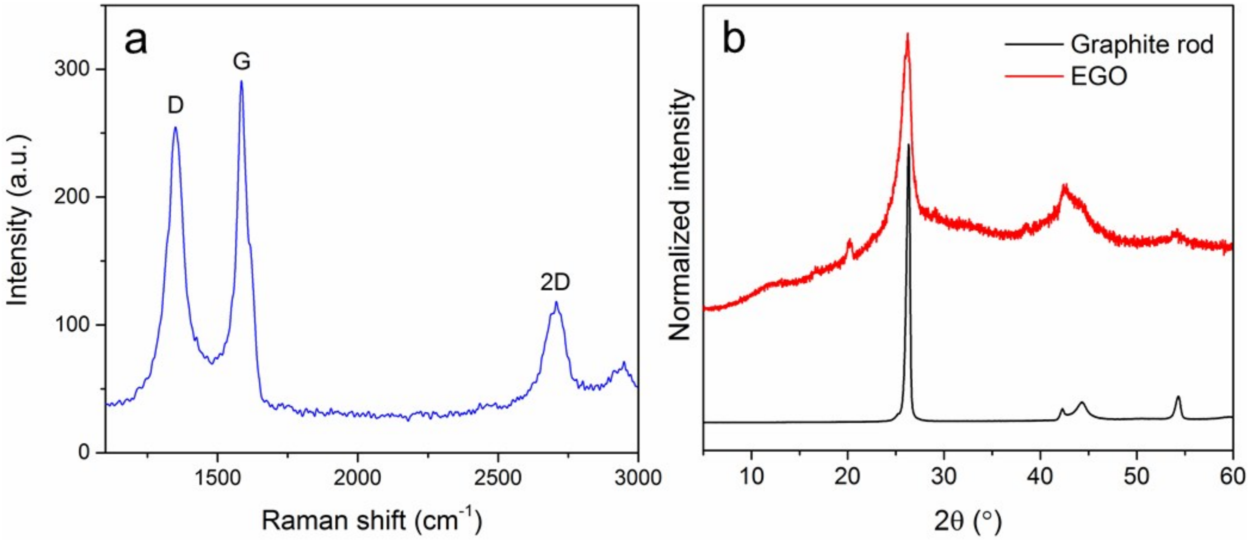

Fig. S6: (a) Raman spectra of EGO. (b) X-ray diffraction (XRD) spectra of graphite rod and EGO.

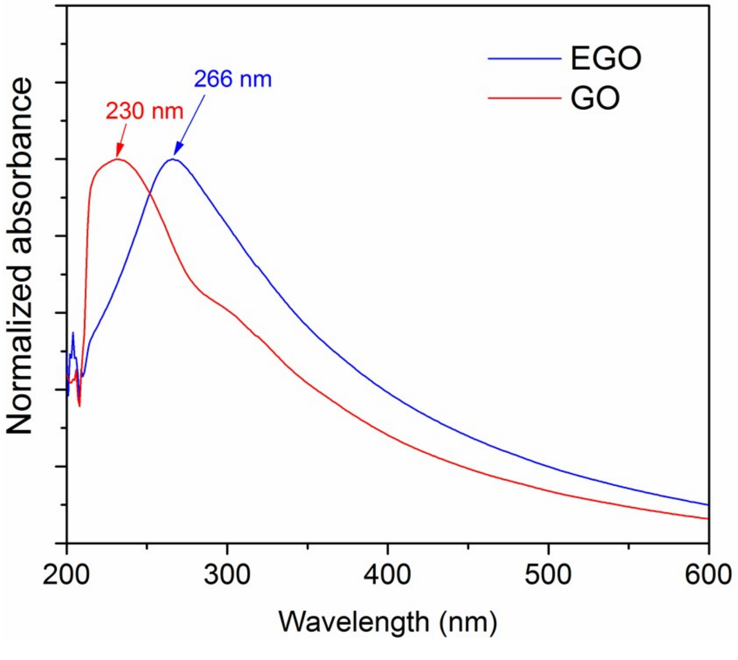

Fig. S7: UV-Visible spectra of EGO and GO in water.

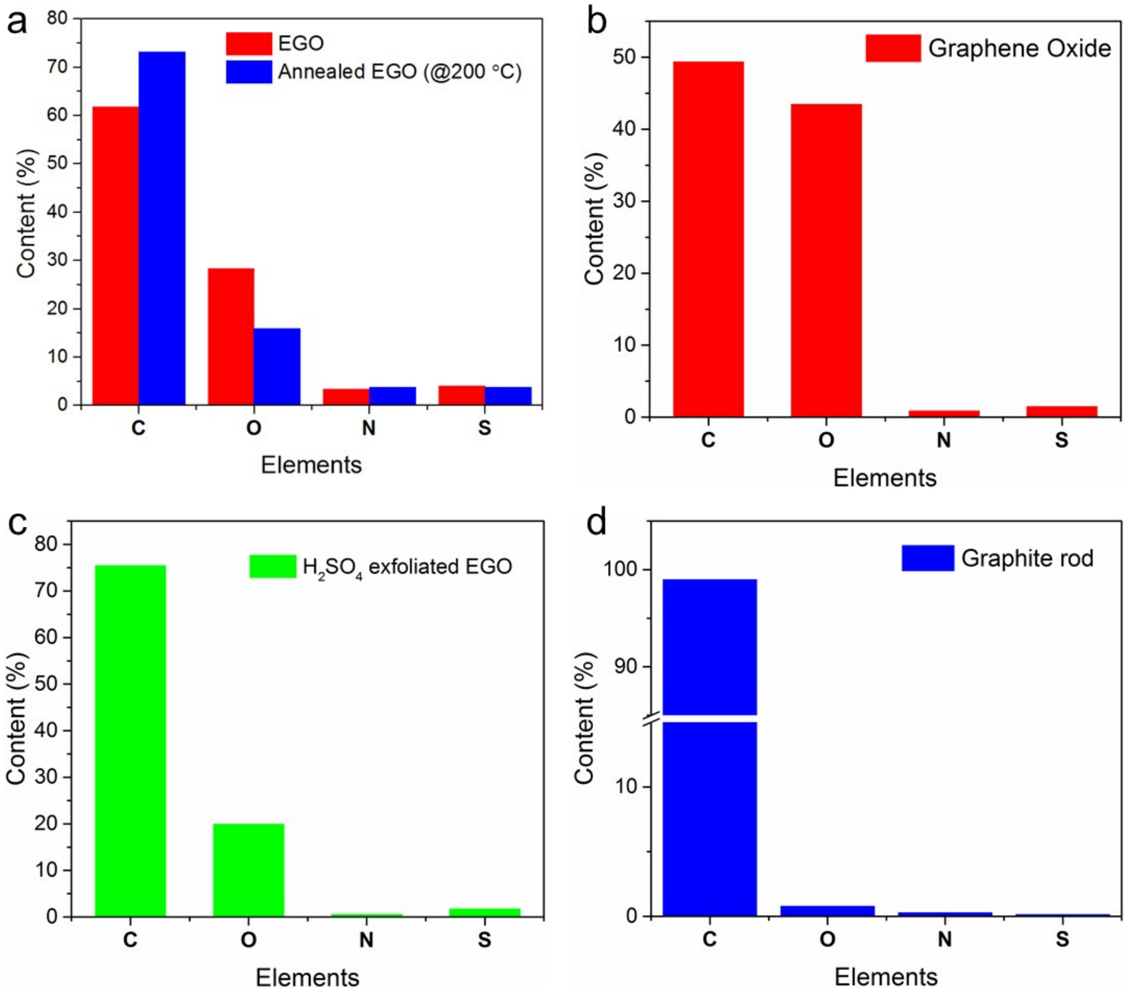

Fig. S8: Elemental analysis of (a) EGO before and after annealing at 200 °C for 2 h, (b) chemically prepared GO, (c) EGO obtained in H_2SO_4 electrolyte and (d) graphite rod used for electrochemical exfoliation, respectively.

As shown in **Fig. S8c**, a small amount of nitrogen was present in the H_2SO_4 exfoliated EGO but the presence of nitrogen is originated from the raw materials that is, graphite rod which contains about 0.3% of nitrogen (**Fig. S8d**).

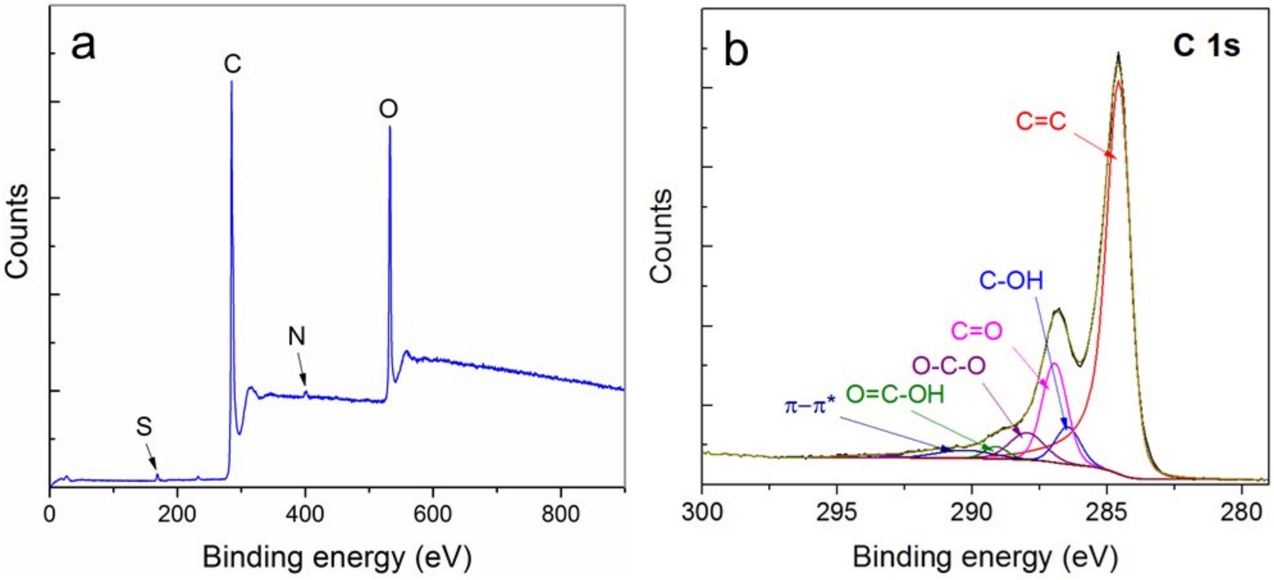

Fig. S9: (a) Wide scan XPS and (b) Deconvoluted XPS spectra of C1s peak of EGO disclosing the presence of 3.43 at% C-OH (286.48 eV), 6.49 at% C=O (286.94 eV), 4.21 at% O-C-O (287.97 eV), 1.98 at% O=C-OH (289.08 eV) and π-π* (290.35 eV) functional groups.

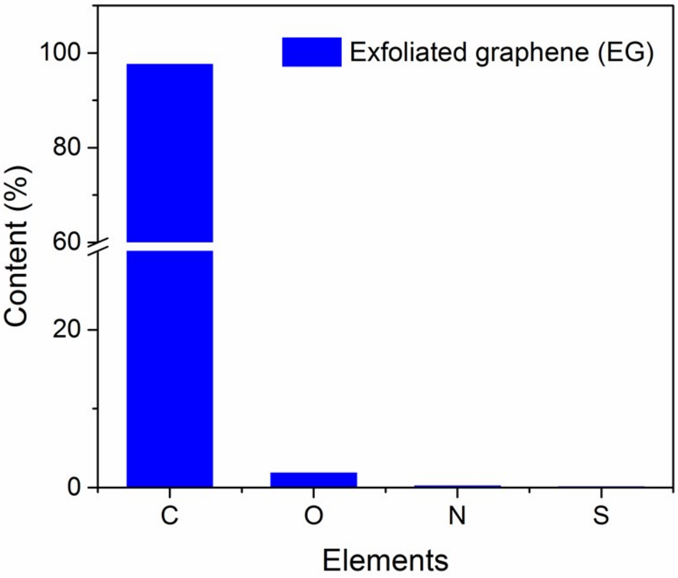

Fig. S10: Elemental analysis of exfoliated graphene obtained from graphite foil.

The chemical composition and properties of electrochemically exfoliated graphene depends on the graphitic material that is used as electrodes. To prove this hypothesis, we also obtained exfoliated graphene using a graphite foil is as a working electrode instead of a graphite rod under the same experimental conditions (i.e. 1.0 M $(NH_4)_2SO_4$, 1.0 A). As shown in **Fig. S9**, the elementals analysis of exfoliated graphene (EG) contains only 1.9% of oxygen and negligible amount of nitrogen (0.25%) and sulfur (0.15%). Therefore, the material can be considered as high-quality graphene. This result is similar to that of reported by Müllen group, where $(NH_4)_2SO_4$ was used as electrolyte and graphite foil and/or flakes were used.[3, 4] On the other hand, as discussed in the main text and shown in **Fig. S8**, the exfoliation of a graphite rod results in much higher oxygen content (i.e. 28.3%) and significant amount of nitrogen and sulfur. This is due to the fact that, the exfoliation of graphite foil occurs very rapidly (usually <20 min) and therefore less time for oxidation and doping. Whereas, a graphite rod exfoliates very slowly (~2 h) compared to the foil which gives longer exposure of the rod to the electrochemical oxidation and doping processes. Thus, the exfoliated graphene obtained from a graphite rod can be considered as graphene oxide (GO) due to its high oxygen content. Nevertheless, these experiments proves that the graphene with different chemical compositions that is, different oxygen content can be obtained via electrochemical exfoliation simply by selecting the right graphite precursor.

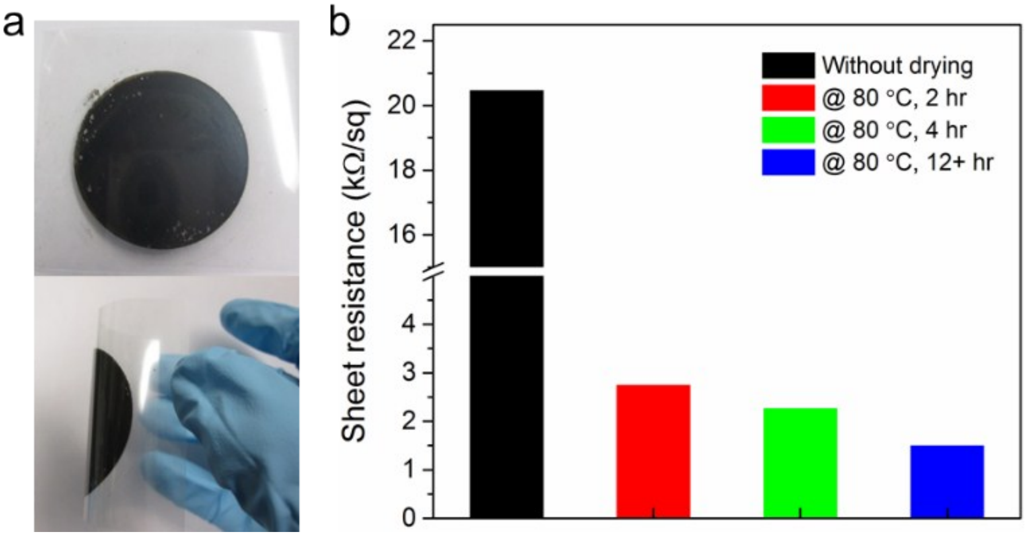

Fig. S11: (a) Photographs of the EGO film on flexible PET substrates fabricated by vacuum filtration and dry transfer method. (b) Changes of sheet resistances of EGO film dried at 80 °C in different time intervals.

Table S1: Effect on graphite exfoliation time with various applied current

Electrode	Electrolyte	Applied current (A)	Exfoliation time
Graphite rod (4.0 cm)	1.0 M $(NH_4)_2SO_4$	1.0	2 h
		0.7	3 h
		0.5	4 h 20 min

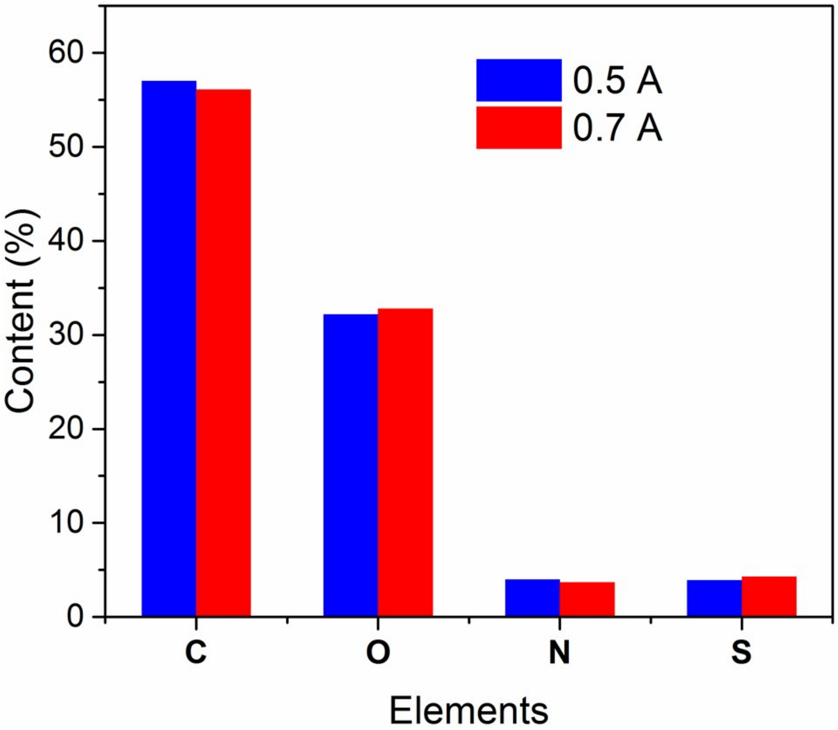

Fig. S12: Elemental analysis of EGO obtained in different applied current.

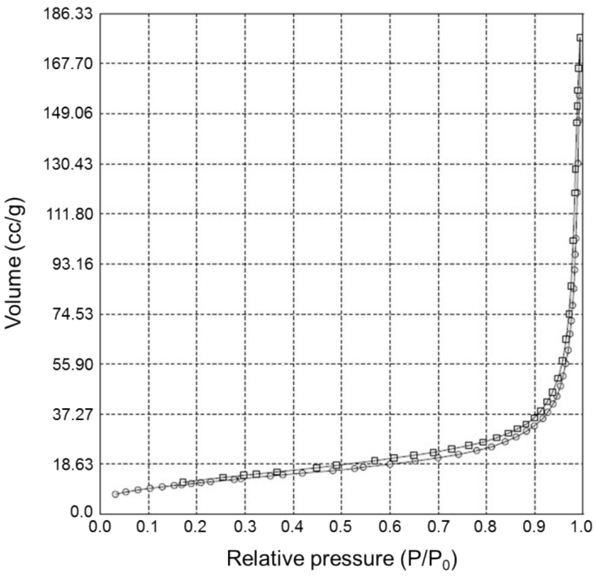

Fig. S13: Nitrogen adsorption-desorption isotherm of EGO powder.

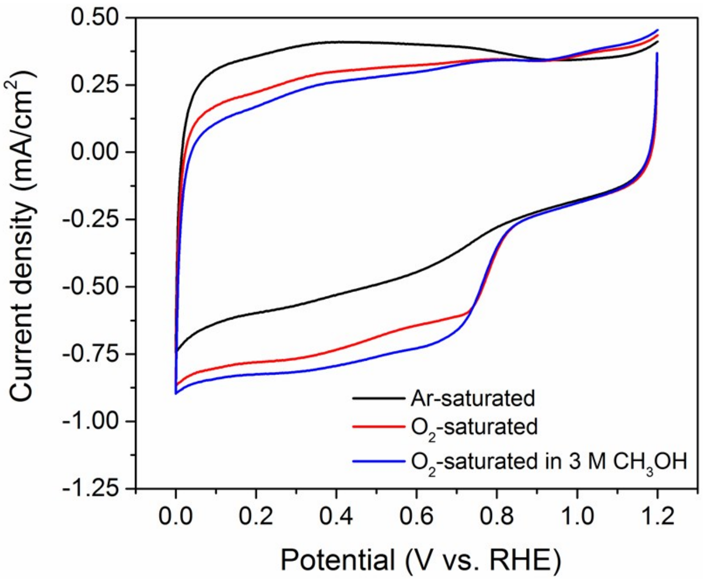

Fig. S14: Cyclic voltammograms of NS-EGO at a scan rate of 50 mV/s in Ar- and O_2-saturated 0.1 M KOH solution as well as O_2-saturated 0.1 M KOH with 3 M CH_3OH.

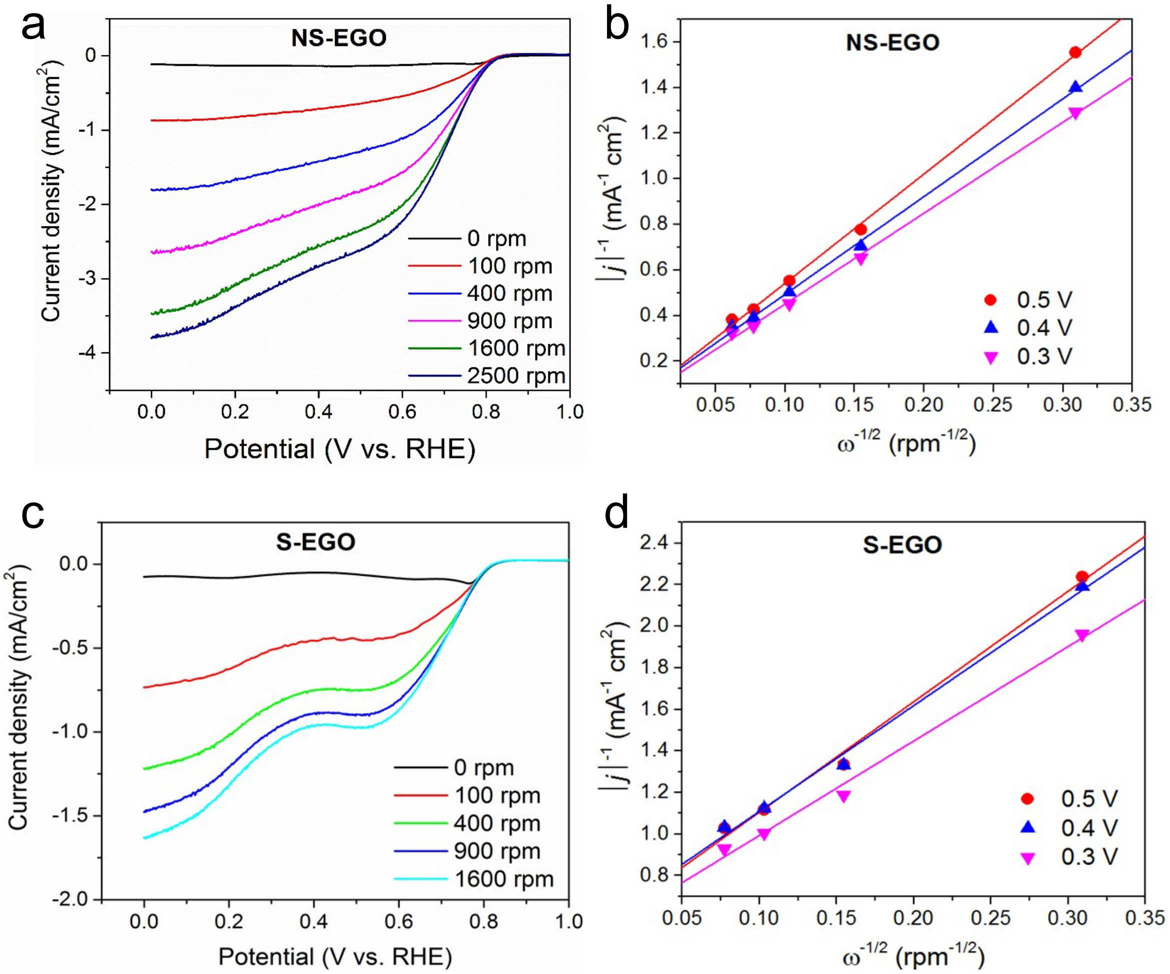

Fig. S15: (a) RDE voltammograms recorded for NS-EGO in an O_2-saturated 0.1 M KOH at a scan rate of 5 mV/s and different rotation rates. (b) Koutecky-Levich (K-L) plot of J^{-1} vs $\omega^{-1/2}$ at potentials of 0.5, 0.4 and 0.3 V *vs*. RHE obtained from (a). (c) RDE voltammograms recorded for S-EGO supported on glassy carbon electrode in an O_2-saturated 0.1 M KOH solution at a scan rate of 5 mV/s and different rotation rates. (d) Koutecky-Levich plot of J^{-1} vs $\omega^{-1/2}$ at different potential obtained from (c).

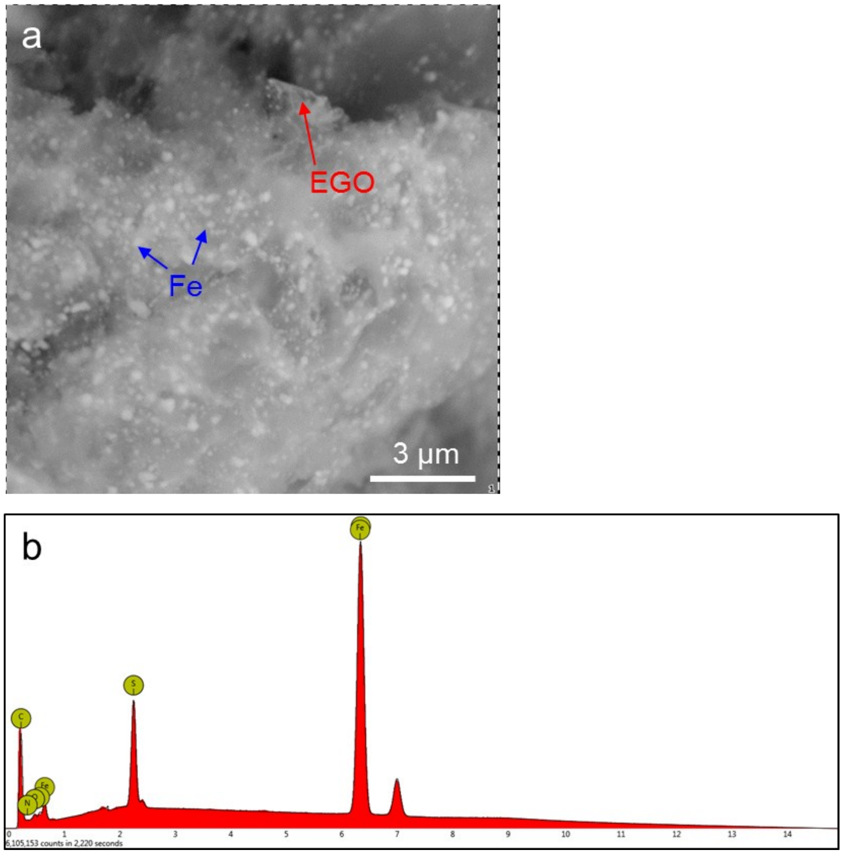

Fig. S16: (a) SEM image of the Fe-NS-EGO composite. (b) EDX of Fe-NS-EGO revealing the presence of different elements (*i.e.* C, O, N, S and Fe) in the composite.

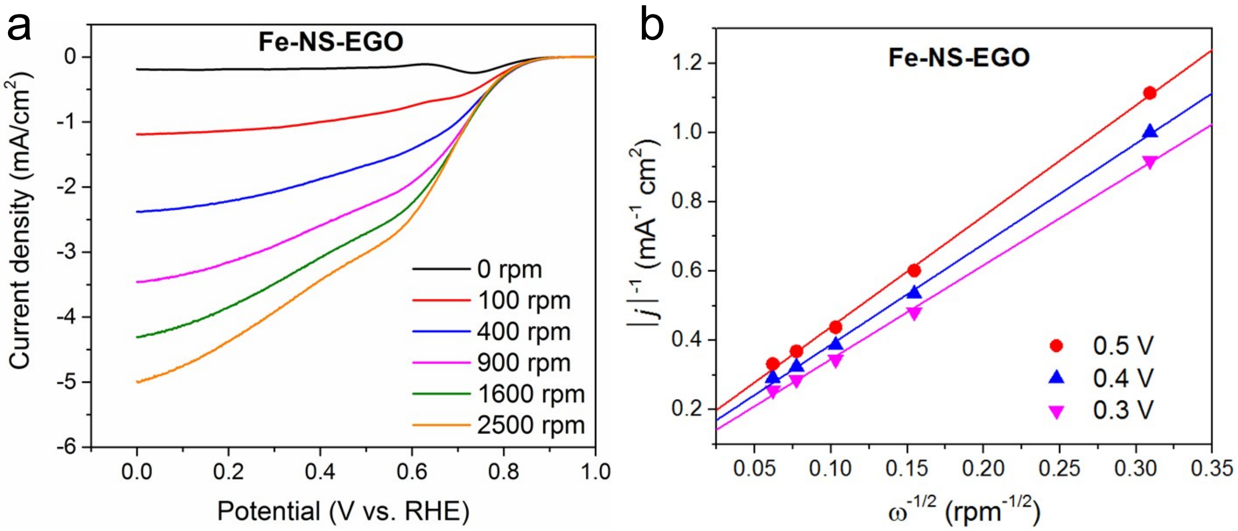

Fig. S17: (a) RDE voltammograms recorded for Fe-NS-EGO in an O_2-saturated 0.1 M KOH at a scan rate of 5 mV/s and different rotation rates. (b) Koutecky-Levich plot of J^{-1} vs $\omega^{-1/2}$ at potentials of 0.5, 0.4 and 0.3 V *vs*. RHE obtained from (a).

Electrochemical ORR properties of S-EGO, NS-EGO and Fe-NS-EGO:

As discussed in the main text and shown in **Fig. S15**, the S-EGO showed significantly lower catalytic performance towards ORR compared to NS-EGO in terms of current density and electron transfer number. The different in the catalytic performance between S-EGO and NS-EGO might be explained with charge or spin densities of the doped graphene. In case of sulfur doped graphene, the sulfur atoms substitute carbon atoms at the graphene sheets in the form of sulfur oxide such as, C-SO_2 and C-SO_3 (**Fig. 3a** in the main text). These sulfur-doped graphene clusters with sulfur oxide locating at the graphene edges show electrocatalytic activity for ORR. Catalytic active sites distribute at the neighboring carbon atoms of doped C-SO_2 or C-SO_3 atoms, which possess large spin or charge density.[5] The sulfur atoms with highest charge density acts as ORR active sites by absorbing O_2 species. On the other hand, when N and S are simultaneously incorporated into graphene, the charge or spin densities are increased to a certain extent indicating higher ORR catalytic performance and providing a synergistic effect.[6] Therefore, the NS-EGO showed higher catalytic activity towards ORR compared to only S-EGO.

The Koutecky-Levich plots were obtained for NS-EGO, S-EGO and Fe-NS-EGO at the kinetic and mixed current regions (**Fig. S15 and S17)**. We observe that a true diffusion-limitation is not achieved for the studied samples, an effect that is pronounced at high rotation speeds. The n values obtained for S-EGO and NS-EGO ranged between 2.0 and 2.6, indicating that peroxide is formed first at lower over-potentials, which is then further partially reduced to water at higher overpotentials. In contrast, the obtained n values for Fe-NS-EGO ranged between 2.8 and 3.4, showing a significant improvement in the electron transfer mechanism, probably due to a faster decomposition of the peroxide intermediate.

References:

1. K. Parvez, R. Li, S. R. Puniredd, Y. Hernandez, F. Hinkel, S. Wang, X. Feng and K. Müllen, *ACS Nano*, 2013, **7**, 3598.
2. K. Parvez, S. Yang, Y. Hernandez, A. Winter, A. Turchanin, X. Feng and K. Müllen, *ACS Nano*, 2012, **6**, 9541.
3. K. Parvez, Z. S. Wu, R. Li, X. Liu, R. Graf, X. Feng and K. Mullen, *J. Am. Chem. Soc.* 2014, **136**, 6083.
4. S. Yang, S. Brüller, Z.-S. Wu, Z. Liu, K. Parvez, R. Dong, F. Richard, P. Samorì, X. Feng and K. Müllen, *J. Am. Chem. Soc.* 2015, **137**, 13927.
5. L. Zhang, J. Niu, M. Li and Z. Xia, *J. Phys. Chem. C* 2014, **118**, 3545.
6. Y. Su, Y. Zhang, X. Zhuang, S. Li, D. Wu, F. Zhang and X. Feng, *Carbon*, 2013, **62**, 296.